RSC Advances

ROYAL SOCIETY OF CHEMISTRY

www.rsc.org/advances

RSC Advances

ARTICLE

Synthesis surface-imprinted Ag nanoplates for detecting organic pollutants in water environment based on surface enhanced Raman scattering

Received 00th January 20xx,
Accepted 00th January 20xx

DOI: 10.1039/x0xx00000x

www.rsc.org/

S. N. Chen,[a] X. Li,*[b,a] S. Han,[a] J. H. Liu[a] and Y. Y. Zhao[c]

Ag-molecularly imprinted polymers (MIPs) hybrid composites (Ag@MIPs) were prepared for the ultra-sensitive detection of organic pollutants in water based on surface enhanced Raman scattering (SERS). The prepared Ag@MIPs hybrid with an about 2 nm ultrathin polymer shell exhibited high affinity. Meanwhile, upon SERS measurements, the limit of detection on Ag@MIPs hybrid can be down to 10^{-12} M for the target molecule Rhodamine B, which was three orders of magnitude higher than classical SERS detections on silver nanoparticles. Furthermore, the Ag@MIPs hybrid also showed good reproducibility and high selectivity toward structurally related analogues. In addition, the present work provides a promising platform for highly sensitive and selective detection of organic pollutants in water based on SERS measurement.

Introduction

The explosion of organic pollutants in water is a very important environmental problem due to their refractory, durability and bioaccumulation.1 Even though in very low concentration, they also have serious threat to aquatic organisms and human health.2-4 The traditional methods to detect organic pollutants include chromatography and bioanalysis.5-6 Chromatography has the advantages of micro amount, rapidity, better accuracy and repeatability, etc., but the pre-treatment process is very complicated.7 As poor stability, bioanalysis often affects the accuracy of testing results.8 Therefore, it is imperative to develop a rapid, accurate, sensitive and reliable method for measuring and monitoring the organic pollutants comprising complicated constituents, similar chemical properties, and low content in polluted water environment.

Surface enhanced Raman scattering (SERS) has become an efficient analysis technique with wide applications, such as biology analysis,[9] material science,[10] catalysis[11] and environmental detection.[12] SERS, an ultra-sensitive spectroscopic probe, can largely enhance Raman signal intensity when excited on the surface of mental materials. It can detect the structure, components, concentrations and some other properties of samples by using spectral fingerprints of molecules based on their characteristic vibrations.[13] More importantly, preparation of high active SERS substrate is the key factor to Raman enhancement.

In past decades, controlling metal nanoparticle structures has attracted considerable attention because of their unique surface plasmon features for SERS. The properties of metal nanoparticles are determined by their composition, size and shape.[14-15] Kelly et al. explored that metal nanoparticles with sharp corners and edges are significant SERS-active substrate, which can markedly improve the local electromagnetic field to enhance the SERS signals.[16] Yang et al. reported that active-substrate with sharp corners and edges is key feature for SERS enhancement in shape-dependent single-particle SERS experiments.[17]

Unfortunately, easy oxidizability and instability are the main drawbacks to the bare metal with good SERS performance.[18] In order to further improve the selectivity, stability and sensitivity of the substrate, researchers have devoted to integrating molecularly imprinted polymers (MIPs) with SERS. Recently, Li et al. produced highly selective detection of bisphenol A on surface-imprinted core-shell Au nanoparticles.[19] Holthoff et al. prepared a nanosensor for 2,4,6-trinitrotolunene (TNT) detection based on MIPs and SERS.[20] Haupt et al. fabricated molecular imprinting-based SERS nanosensors.[21] Our group also prepared Ag@MIP hybrid nanostructures with high detection sensitivity based on MIP-SERS.[22-23] One advantage is that MIPs can specifically and selectively recognize the target molecule. Another advantage is that MIPs coated on the surface of mental can prevent oxidation and keep stabilization. Although these related reports are seldom available, the excellent properties of MIPs still show a perfect application prospect in SERS fields.

In this study, we fabricated triangle/hexagon Ag@MIPs hybrid nanoplates to detect organic pollutants. The preparation process and SERS performance of Ag@MIPs are shown in Fig.1. Triangle/hexagon Ag nanoplates were obtained by solvothermal method, and were then modified by MPS to synthesis Ag-MPS under the room temperature. Then, methacrylamide and DVB were

[a] Department of Chemistry, Harbin Institute of Technology, Harbin 150001,P. R. China.
[b] State Key Lab of Urban Water Resource and Environment, Harbin Institute of Technology, Harbin 150090, PR China. E-mail: lixin@hit.edu.cn
[c] College of Chemistry , Jilin Normal University, Siping,136000, PR China.
*Corresponding author. Fax: +86 451 86282153. Tel: +86 451 86282153.
E-mail address: lixin@hit.edu.cn (X. Li)

polymerized at the presence of RhB to form a MIPs layer coated on the surface of Ag-MPS, and the target molecule (Rhodamine B, RhB) was removed by methanol-acetic acid solution to form Ag@MIPs with memory cavities. Herein, Ag@MIPs could be used for sensitivity and specificity detection of RhB. The results show that the Ag@MIP nanoplates exhibit high detection sensitivity (10^{-12} M), and can be reused for the detection of the target molecules.

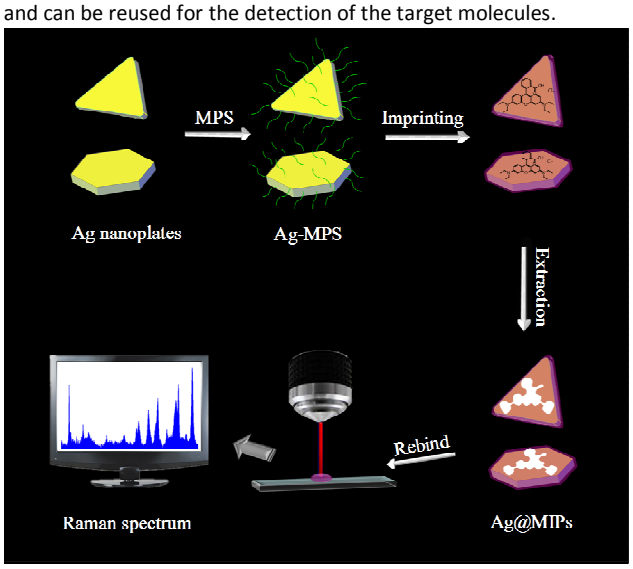

Fig.1. Schematic illustration of the preparing process of Ag@MIPs for detecting RhB by SERS.

Experimental Section

Chemicals and materials.

N, N-dimeth-ylformamide (DMF) was purchased from Guoyao Chemical Reagent (Shanghai, China). Silver nitrate ($AgNO_3$), methanol, and acetic acid were purchased from the Tianda Chemical Reagent Plant (Tianjin, China). 3-Methacryloxypropyltrimethoxysilane (MPS) was obtained from Aladdin. Methacrylamide, Azobisisobutyronitrile (AIBN), and divinylbenzene (DVB) were obtained from Guangfu Chemical Industry (Tianjin, China). Acetonitrile was purchased from the Third Chemical Factory of Tianjin (Tianjin, China). Poly(vinyl pyrrolidone) (PVP-K30) was imported from the United States. Rhodamine B (RhB) was obtained from Sigma-Aldrich.

Synthesis of Ag nanoplates.

Ag nanoplates with small size distribution were prepared by a seedless solvothermal reduction method. First, PVP (320mg) and $AgNO_3$ (320mg) were dissolved in 10ml DMF separately. Next, HCl (0.75 μL) was dropped into DMF (40 ml) after heated for 30 min in the 140°C oil bath. The two precursor solutions were injected into the hot reaction flask simultaneously, and the reaction mixture was stirred at 140°C for 8 h. After cooling, the product was collected and washed several times with ethanol by centrifugation (at 10000 rpm). Finally, Ag nanoplates were dried under vacuum at 40°C for 24h.

Synthesis of MPS modified Ag nanoplates (Ag-MPS).

200 mg Ag nanoplates were dispersed in 20 ml ethanol-ultrapure water (4:1, v/v) solution by ultrasound treatment for 15 min. After 2 ml MPS was then dropped into reaction flask under nitrogen protection, the mixture was stirred at room temperature for 16 h. The product was dried under vacuum at 40°C for 24h.

Synthesis of Ag@MIPs hybrid nanoplates.

100 mg RhB (template molecules), 1.42 ml DVB (cross-linking agent), 215 mg Methacrylamide (functional monomer), and 10 mg AIBN were dissolved in 20 ml acetonitrile. Then 100 mg Ag-MPS nanoplates were dispersed into mixture by ultrasonic treatment for 30 minutes. In order to make ultrathin MIPs shell, the reaction was vigorously stirred 12 h at 60 °C under nitrogen protection. The product was washed with methanol-acetic acid (4:1, V/V) solution until no template molecule was detected in the washing solutions. Finally, core-shell Ag@MIPs nanoplates were dried under vacuum at 40 °C for 24 h.

Characterization.

Crystallographic structure of products was characterized by X-ray diffractometer (XRD, Shimadzu XRD-6000) with Cu Kα radiation (λ =1.5406 Å). The structural groups of the composite were analyzed by Fourier transform infrared spectrometer (FT-IR, Avatar 360). Surface element compositions were gained by X-ray photoelectron spectroscopy (XPS, VG ESCALAB Mark II). The structure and surface morphology of the nanoplates were measured by Transmission electron microscope (TEM, Tecnai G20 Philip) and scanning electron microscopy (SEM, FEI HELIOS NanoLab 600i). Raman spectra were recorded on a Renishaw in Via micro-Raman spectroscopy system (λ = 633 nm). The available laser power kept at 0.69 μ W, and accumulation time was 1 s.

Results and discussion

Ag nanoplates were fabricated by one-step solvothermal reduction of AgNO3 in the presence of DMF and PVP. Fig. 2a and b show low- and high-magnification scanning electron microscopy (SEM) image of the Ag nanoplates. It can be clearly observed that high quantity triangle/hexagon Ag nanoplates have been obtained. A piece of vertical Ag nanoplate is observed in Fig. 2b, and its thickness is about 40.5 nm. The average diameter of triangle/hexagon Ag nanoplates is calculated about 250 nm from the SEM images. Comparing with the nanoplate products reported by Liz-Marzán,24 all of Ag nanoparticles all have plate structure and well disperse with small size distribution in our method. MIPs layer grow on the surface of the triangle/hexagon Ag nanoplates can be confirmed by TEM in Fig.2c, and MIPs layer in Fig.2d approximates 2 nm which can enhance the stability of active-SERS substrate.25 The Ultrathin MIPs layer could improve the selectivity to overcome the similar compounds,19 and avoid RhB molecules directly touching the surface of Ag nanoplates.

The structures of Ag nanoplates and Ag@MIPs were recorded by using XRD analysis. As displayed in Fig.3, the XRD patterns of Ag nanoplates have four intensive diffraction peak located at 38.12°, 44.26°, 64.41°, 77.36°, which can well correspond to (111), (200), (220) and (311) crystal planes of face-centered cubic (fcc) Ag in the card (JCPDS File No. 04-0783). After MIPs layer was encapsulated on the surface of Ag-core, the intensity of Ag@MIPs diffraction peaks became weaker. But the characteristic peak positions of Ag@MIPs well correspond to the Ag nanoplates, suggesting successful synthesis of Ag@MIPs.

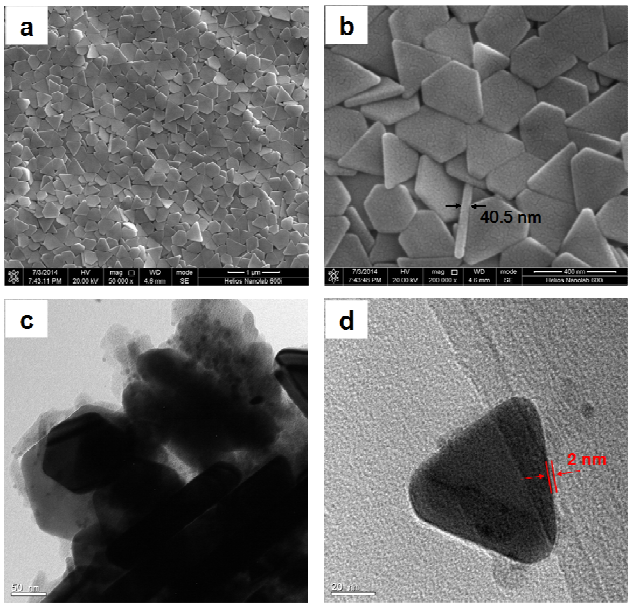

Fig.2. (a) Low- and (b) high-magnification SEM images of reduced Ag nanoplates. (c) Low- and (d) high-magnification TEM images of Ag@MIPs.

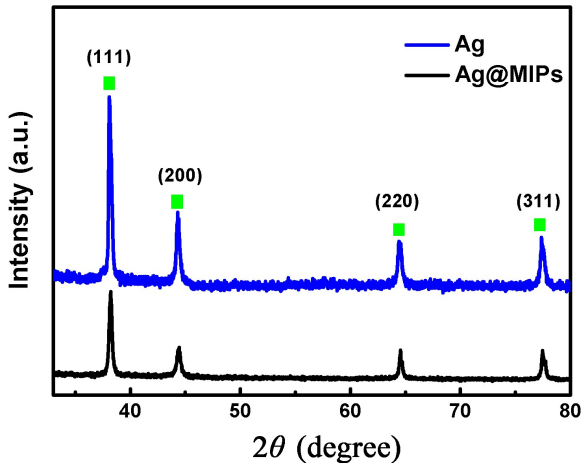

Fig.3. XRD patterns of Ag nanoplates and Ag@MIPs.

EDS analysis of Ag nanoplates, Ag-MPS, and Ag@MIPs has also been studied. From Fig.4a, we could see that Ag element appears in the EDS spectrum of Ag nanoplates. After the Ag nanoplates were modified by MPS, the signals of Si, Ag elements then appear in the EDS spectrum of Ag-MPS, which is shown in Fig.4b. This result shows that MPS have been grafted onto the surface of the Ag nanoplates. In Fig.4c, EDS spectrum of Ag@MIPs indicates the presence of C, O, and Ag elements, but Si element has disappeared. This is because Ag-MPS nanoplates are encapsulated by MIP layer. These results suggest that the MIPs layer was already fabricated on the surface of Ag nanoplates.

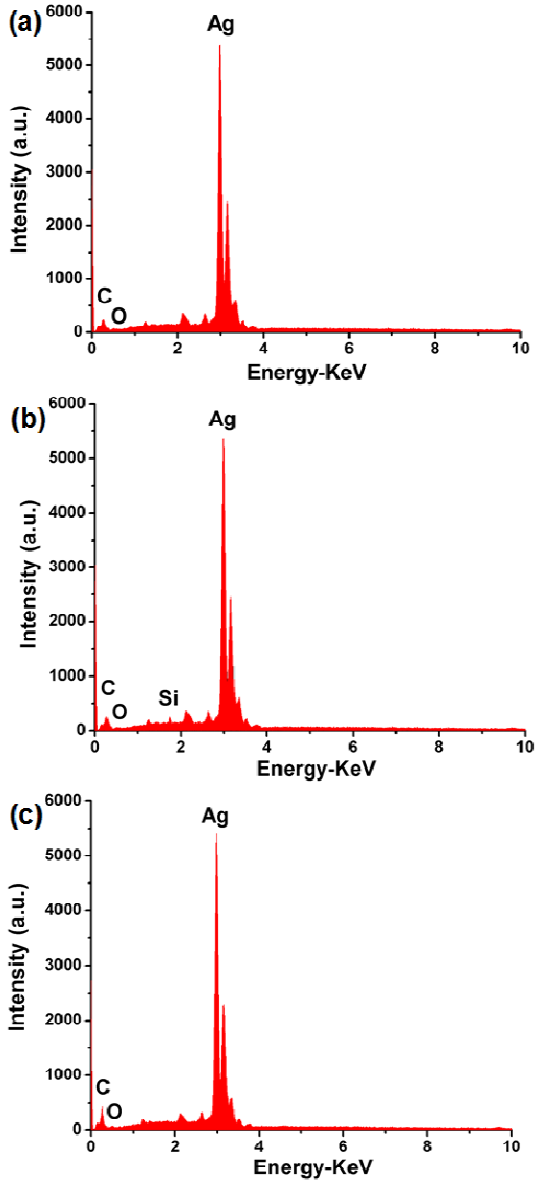

Fig.4. EDS spectra of (a) Ag nanoplates, (b) Ag-MPS, and (c) Ag@MIPs.

To futher prove that MIPs layer has been coated onto the surface of Ag nanoplates, FT-IR is employed to characterize Ag nanoplates, Ag-MPS, Ag@MIPs (Fig.5). As shown in curve a, the bending vibration peaks at 3432.31cm^{-1} and 1628.90 cm^{-1} resulting from O-H vibration. The absorption band of Ag nanoplates around 2920.40 cm^{-1} is attributed to the C-H of -CH_3 for DMF. In curve b, the feature of the Ag-MPS is C=O band around 1665.16 cm^{-1}, which indicated that MPS has been successfully modified to Ag nanoplates surface. As the MIPs layer coated on the surface of Ag nanoplates, the peaks of Ag@MIPs become weak compared with Ag nanoplates in curve c. The vibration peak around 1201.16 cm^{-1} is attributed to the C-N- of RhB. It further indicates that Ag@MIPs has been successfully prepared.

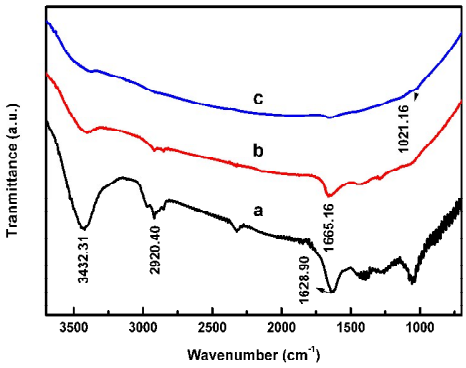

Fig.5. FI-IR spectra of Ag nanoplates (a), Ag-MPS (b), and Ag@MIPs (c).

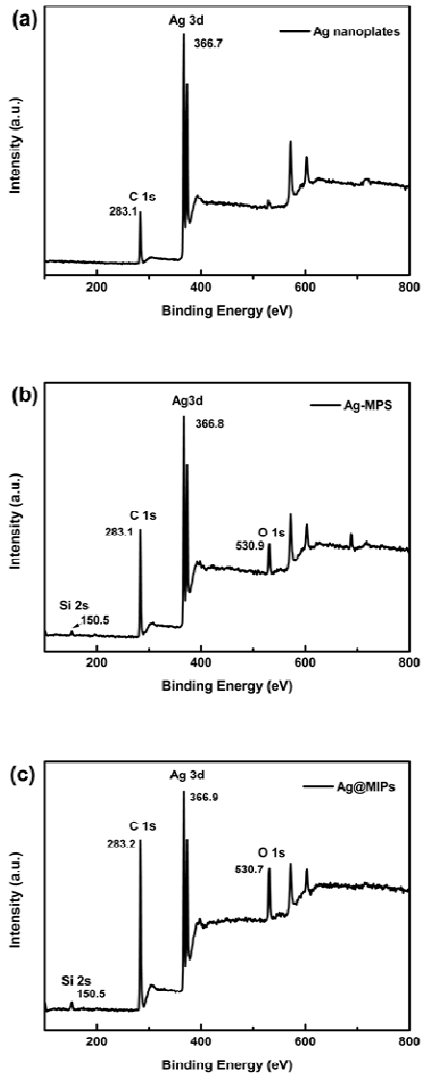

Fig.6. XPS spectra of Ag nanoplates (a), Ag-MPS (b), and Ag@MIPs (c).

In order to verify the existence of MIPs layer, the X-ray photoelectron spectra (XPS) of Ag nanoplates, Ag-MPS and Ag@MIPs were measured in Fig.6. From Fig.6a, we can observe chemical binding energies at approximately 283.1 and 366.7 eV for C 1s and Ag 3d, respectively. C element comes from unwashed PVP on the surface of Ag nanoplates. The XPS spectrum of Ag-MPS contains the new peak at approximately 150.5 eV which is assigned to the energies of Si 2s, and it confirms that MPS is grafted on the Ag nanoplate surface in Fig.6b. As shown in Fig.6c, the contents of C and O elements increased because of the MIPs layer coated onto the Ag-MPS surface. The results show that the Ag@MIPs were successfully prepared.

Equilibrium binding experiments were carried out to evaluate the binding ability of the Ag@MIPs (a) and Ag (b). The sorption isotherms of RhB on Ag@MIPs and Ag are presented in Fig.7. Because of MIP layer with imprinted cavities which can gather organic pollutants and concentrate target molecules, Ag@MIPs exhibits excellent adsorption performance.

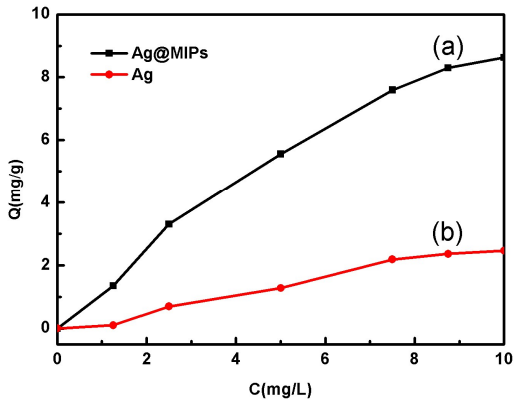

Fig.7. Adsorption isotherms of Ag@MIPs (a) and Ag(b).

Organic pollutants, such as RhB, are chosen as a probe molecule to reveal the SERS activity of Ag nanoplates and Ag@MIPs. After being soaked in RhB solution with different concentrations for 2h, the SERS spectra collected from Ag nanoplates and Ag@MIPs substrates are shown in Fig.8. The SERS spectra of RhB are consistent with previous report.[26] As shown in Fig.8, the bands at about 1279cm^{-1}, 1357cm^{-1}, and 1647cm^{-1} are assigned to aromatic stretch vibrations. The bands approximately at 620cm^{-1} and 1195cm^{-1} are associated with ring deformation and C-H inplane bend vibrations, respectively. And the strong band at 1529cm^{-1} is recognized as C-H vibration characteristic peaks. With the decreasing of RhB concentration, the Raman peaks of RhB on Ag@MIPs and Ag nanoplates gradually decreased, but the location of Raman characteristic peaks are not drifted. In Fig.8a, the Raman spectrum of extracted Ag@MIPs has some weak background interference, but the feature characteristics of RhB SERS spectra also can be identified clearly by Ag@MIPs substrate even at a concentration as low as 10^{-12} M. According to our previous report,[27] the enhancement factor (EF) can be estimated to be 1.01×10^{7} at 1647 cm^{-1}. The minimum concentration of RhB solution detected with Ag nanoplates is 10^{-9} M in Fig.8b. It can be seen that the

limiting detectable concentration of the Ag@MIPs substrate has been improved by three orders of magnitude when compared with the Ag nanoplates. The results implied that MIPs layer encapsulated on the surface of Ag nanoplates, as an effective SERS substrate, can enhance the SERS activity and have potentials for detecting probe molecule.

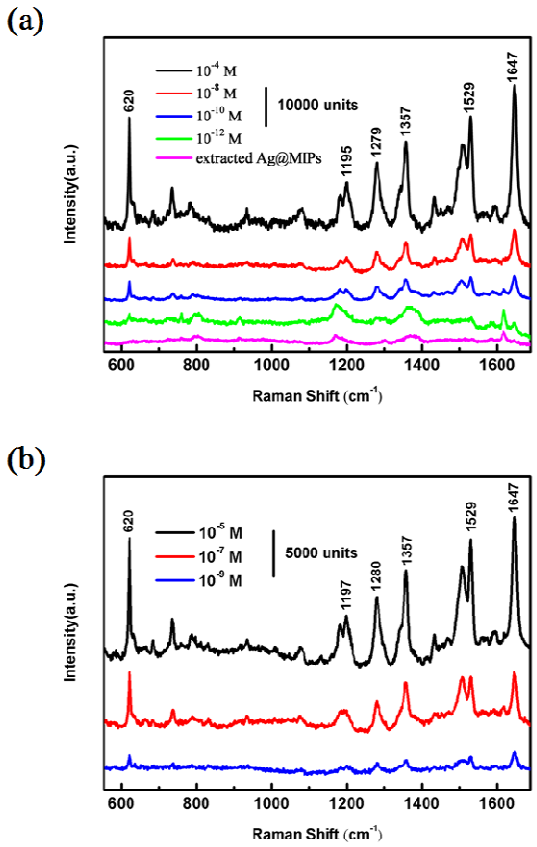

Fig.8. SERS spectra of (a) Ag@MIPs and (b) Ag nanoplates in different concentrations RhB solution.

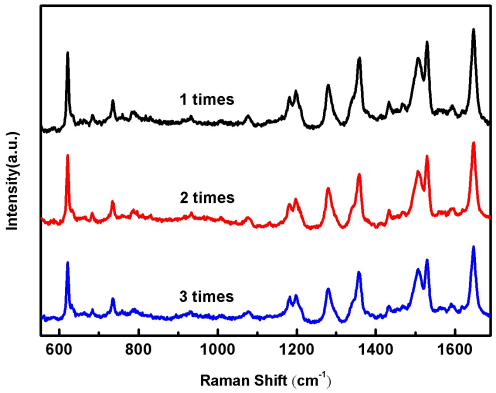

Fig.9. The regeneration performance of the Ag@MIPs.

The Raman spectra of RhB are showed in Fig.9 on the reusable Ag@MIPs. The repeatability of Ag@MIPs is investigated in 10^{-5} M RhB water solution for 2 h. The used Ag@MIPs were extracted by methanol-acetic acid solution, and then circularly used for 3 times. Although the Ag@MIPs memory cavities were partly destroyed during the regeneration process, the intensity of RhB Raman spectra was not obviously decreased in SERS enhancement. Therefore, our synthetic materials present excellent regeneration capability.

MIPs with imprinted cavities have specific recognition capacity toward the template molecules. Due to similar molecular structures with Rhodamine B, Rhodamine 6G and Methylene blue were selected for investigating the recognition of Ag@MIPs. The selectivity of Ag@MIPs was studied in 10^{-5} M Rhodamine B, Rhodamine 6G and Methylene blue solution for 2 h. Compared with two other molecules, RhB shows stronger SERS enhancement on the Ag@MIPs in Fig.10. This phenomenon confirms that the MIP layer can reflect its advantage when coating on the surface of Ag nanoplates. The results imply that MIPs can improve sensitivity of Raman spectra as a crucial factor for SERS.

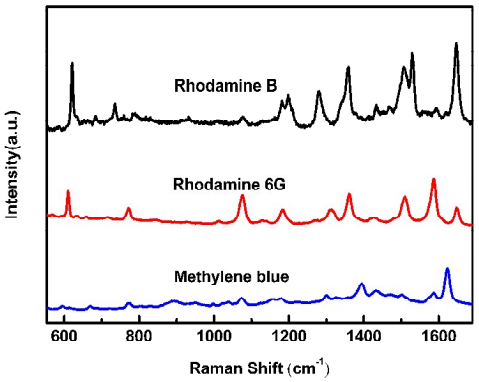

Fig.10. SERS spectra of Rhodamine B, Rhodamine 6G and Methylene blue recorded from Ag@MIPs at a concentration of 10^{-5} M.

Generally, SERS enhancement is attributed to the Chemical (CM) and Electromagnetic (EM) mechanism. EM enhancement is a main factor for long-range enhancement effects.[28] In other words, Raman signals can be detected further away from the SERS substrate surface. However, CM enhancement is a short-range effects,[29] which generated by the target molecules interacting with the SERS substrate surface.

In our case, the enhancement mechanism of Ag@MIPs with highly sensitive SERS performance may has two contributing factors. Firstly, one possible reason is that the high SERS signals relate to the creation of SERS hot spots. Hot spots require exceedingly small structures and gaps to further improve typically high SERS activity.[30-31] Ag@MIPs surface leaves three-dimensional cavities corresponding hole sizes and chemical bonds matched with the template molecules. As these cavities may arrange orderly and connect closely with small gap in the MIP layer, the hot spots effect are strengthened when the template located in the cavities interacts with Ag nanoplates. Secondly, we have prepared 2 nm ultrathin MIPs layer obtaining well Raman signals, which conforms

the long-range effect of the EM enhancement mechanism. Tian et al. have demonstrated that strong SERS enhancement is existing when the ultrathin coating of the SERS substrate is less than 2 nm thick.[32] According the above discussions, the Raman enhancement is attributed to the combination of CM and EM in our system.

Conclusions

In the present study, an effective strategy for selective and sensitive detection of organic pollutants in water has been developed through synthesis of Ag@MIPs hybrid as an active SERS substrate. The detection limit for RhB can down to 10-12 M, which was three orders of magnitude higher than classical SERS detections on Ag nanoparticles. Moreover, the Ag@MIPs hybrid exhibited good reproducibility and high selectivity to structurally related analogues. This originates from both the structure features of ultra-thin MIPs layer and Ag nanoplates. This developed approach opens up intriguing potential for detecting organic pollutants in water.

Acknowledgements

This study was supported by the National Natural Science Foundation of China (No. 21176052,51379052 and 51579057), the State Key Laboratory of Urban Water Resource and Environment, Harbin Institute of Technology (2013TS05), and the Program for Innovation Research of Science in the Harbin Institute of Technology.

References

1. Z. Hasan and S. H. Jhung, *J. Hazard Mater.*, 2015, **283**, 329.
2. F. Wania, and D. Mackay, *Environ. Sci. Technol.* 1996,**30**, 390A.
3. D. Li, Q. Zhu, C. Han, Y. Yang, W. Jiang, and Z. Zhang, *J. Hazard Mater.*, 2015, **285**, 398.
4. Hernández F, Ibáñez M, Portolés T, M. I. Cervera, J. V. Sancho, and F. J. López, *J. Hazard Mater.*, 2015, **282**, 86.
5. K. Lüthje, T. Hyötyläinen, and M. L. Riekkola, *Anal. Bioanal. Chem.*, 2004, **378**, 1991.
6. M. Farré, L. Kantiani, M. Petrovic, S. Pérez, and D. Barceló, *J. Chromatogr. A*, 2012, **1259**, 86.
7. X. H. Chen, L. X. Zhou, Y. G. Zhao, S. D. Pan, and M. C. Jin, *Talanta*, 2014, **119**,187.
8. Z. Dai , and H. Ju, *TRAC-Trend. Anal. Chem.*, 2012, **39,** 149.
9. D. Podlipna, and M. Cichna-Markl, *Eur. Food Res. Tenchnol.*, 2007, **224**, 629.
10. C. Zhu, G. Meng, Q. Huang, and Z. Huang, *J. Hazard Mater.*, 2012, **211**, 389.
11. D. Y. Wu, X. M. Liu, Y. F. Huang, B. Ren, X. Xu, and Z. Q. Tian, *J. Phys. Chem. C*, 2009, **113**, 18212.
12. Z. Y. Bao, X. Liu, Y. Chen, Y. Wu, H. L. Chan, J. Dai, and D. Y. Lei, *J. Hazard Mater.*, 2014, **280**, 706.
13. C. G. Boeriu, D. Bravo, R. J. Gosselink, and J. E. van Dam, *Ind. Crops Prod.*, 2004, **20**, 205.
14. M. A. El-Sayed, *Accounts Chem. Res.*, 2001, **34**, 257.
15. J. B. Jackson, and N. J. Halas, *J. Phys. Chem. B*, 2001, **105**, 2743.
16. K. L. Kelly, E. Coronado, L. L. Zhao, and G. C. Schatz, *J. Phys. Chem. B*, 2003, **107**, 668.
17. Y. Yang, S. Matsubara, L.Xiong, T. Hayakawa, and M. Nogami, *J.Phys. Chem. C*, 2007, **111**, 9095.
18. S. Chen , X Li , Y. Zhao , L. Chang, and J. Qi, *Carbon*, 2015, **81**,767.
19. J. Q. Xue, D. W. Li, L. L. Qu, and Y. T. Long, *Anal. Chim. Acta*, 2013, **777**, 57.
20. L. Yang, L. Ma, G. Chen, J. Liu, and Z. Q. Tian, *J. Chem. Eur.*, 2010, **16**, 12683.
21. M. Bompart, Y. De Wilde, and K. Haupt, *Adv. Mater.*, 2010, **22**, 2343.
22. L. Chang, Y. Ding, and X. Li, *Biosensors and Bioelectronics*, 2013, **50**, 106.
23. S. Chen, X. Li , Y. Guo, and J. Qi, *Analyst*, 2015, **104**, 3239.
24. I. Pastoriza-Santos, and L. M. Liz-Marzaán, *Adv. Funct. Mater.*, 2009, **19**, 679.
25. F. Yang, Q. Wang, Z. Gu, K. Fang, G. Marriott and N. Gu, *ACS Appl. Mater. Interfaces*, 2013, **5**, 9217.
26. J. Fu, Z. Cao, and L. Yobas, *Nanotechnology*, 2011, **22**, 505302.
27. S. Chen, X. Li, Y. Zhao, L. Chang and J. Qi, *Chem. Comm.*, 2014, **50**, 14331.
28. A. Campion, and P. Kambhampati, *Chem. Soc. Rev.*, 1998, **27**, 241-250.
29. R. Olivares-Amaya, D. Rappoport, P. A. Munoz, P. Peng, E. Mazur, and A. Aspuru-Guzik, *J. Phys. Chem. C*, 2012, **116**, 15568.
30. G. Braun, I. Pavel, A. R. Morrill, D. S. Seferos, G. C. Bazan, N. O. Reich, and M. Moskovits, *J. Am. Chem. Soc.*,2007, **129**, 7760.
31. L. Qin, S. Zou, C. Xue, A. Atkinson, G. C. Schatz, and C. A. Mirkin, *Proc. Natl. Acad. Sci. U S A*, 2006, **103**, 13300.
32. J. Li, Y. Huang, Y. Ding, Z. Yang, S. Li, X. Zhou, F. Fan, W. Zhang, Z. Zhou, D. Wu, B. Ren, Z. Wang, and Z. Tian, *Nature*, 2010, **464**, 392.